# UNIVERSITY OF TWENTE.

## Faculty of Science and Technology

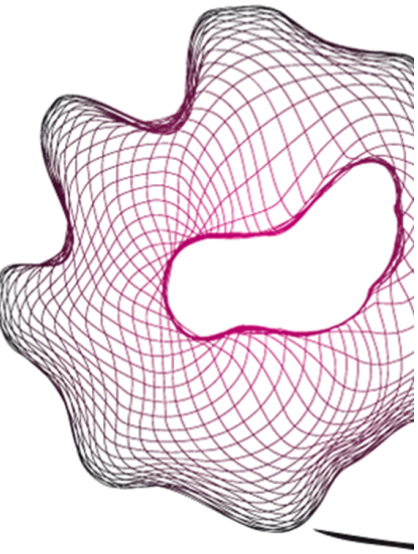

# Measurement of the velocity and viscosity of fluids in a micro channel with Optical Coherence Tomography

**Harm T. M. Wiegerinck**

**Bachelor's Thesis**

**July 2017**

**Comittee:**
**Daily Supervisor:**
K.E. El Obied MSc.
**Responsible Teacher:**
Prof. dr. ir. R.G.H. Lammertink
**Member Examination Board:**
Dr. ir. D.W.F Brilman

Soft Matter, Interfaces and Fluidics Group
Faculty of Science and Technology
University of Twente
P.O. Box 217
7500 AE Enschede
The Netherlands

**Abstract**

The growth of bacterial biofilms in water treatment membrane units is a serious problem, which makes the membrane process less efficient and more expensive, therefore more research must be done to reduce and manage the formation of a biofilm by tuning the operating conditions such as the flow. One of the problems is the viscoelastic nature of biofilms, therefore the viscosity and viscoelastic parameters should be studied non-invasively and during flow . This could in principle be done in a cylindrical glass capillary optically with Optical Coherence Tomography (OCT). So far this has only been studied with a water flow. Therefore in this Thesis a model compound, that could also be found in biofilms, called xanthan gum is used. The measurement of the viscosity has been done with and without flow through the capillary. For the no flow measurements the Stokes-Einstein equation and a microrheology model have been used in order to get information on the viscosity and viscoelastic parameters. For the flow experiments a two parameter fit was used to obtain the velocity and viscosity of the fluid flows simultaneously. From the no-flow experiments it can be concluded that microrheology can be used to obtain a trend in the viscosity which correspond to high shear rates and from the flow experiments it can be concluded that the velocity profile can be measured quite well and the viscosity profile as function of shear rate can only be obtained by combining results from different flow rates. With these findings it becomes more clear how the OCT could potentially be used in future research to measure the viscosity of biofilms under operating conditions in a micro channel.

# Contents

# 1 Introduction

## 1.1 Problem Statement

Membranes are often used in the treatment of water, for example to desalinate seawater or to clean wastewater. The problem with membranes is that the pores can become blocked by particles or (in)organic substances,which is called membrane fouling. A special type of fouling is biofouling, this is caused by the growth of microorganisms on the surface of the membrane and membrane spacers.

Almost all water contains microorganisms such as algae or bacteria, which are able to attach to the surface of a membrane and reproduce on the surface. As the amount of microorganisms grows, they begin to excrete extracellular polymeric substances (EPS), which makes attachment of other species to the surface more favorable. This process leads to a slimy layer that consists of bacteria, EPS and water on the membrane, which is called a biofilm. Because of the reproduction of the microorganisms this problem even occurs when most of the microorganisms are removed before the water is purified by the membrane.[1] When a biofilm is present on a surface for a while, the biofilm matures and disperses single cells with biofilm material away from the biofilm. These cells can attach to another surface to repeat the whole cycle again inside the membrane. This cycle can be seen schematically in Figure 1.1 [2]

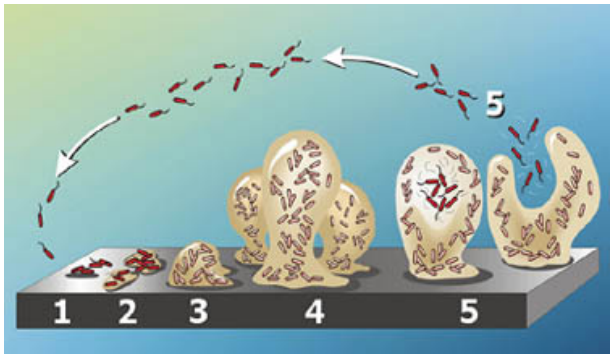


Figure 1.1: *Growth phases of a biofilm. Source:[3]*

The biofilm is an extra barrier on top of the membrane, so the growth of the biofilm leads to a decline in membrane flux and this makes the process less efficient. The energy consumption also increases due to a biofilm, especially when the biofilm grows across the feed channel, because this increases the flow resistance. This means that there is a higher pressure drop over the membrane, so more power is required to pump water through the membrane to maintain the same flow.[1]

In order to remove the biofilm the membrane must be cleaned, which takes time and sometimes even the complete membrane unit has to be replaced, which makes a membrane process for water treatment more expensive.

It is therefore essential to study the properties of the biofilm as the biofilm is subjected to various operating conditions such as a the flow rate or the effect of the addition of various antimicrobials. One of the problems related to flow are the viscoelastic properties of the biofilm,because this means it reacts to shear stress of the water by a combination of elastic and viscous deformation, which means it can recoil back into the same position and deform irreversibly. When a biofilm is more elastic it is obviously harder to remove and therefore the viscosity and viscoelastic properties are important parameters to study the effect on the biofilm of certain conditions.[4]

In the past the viscosity of biofilms was often studied by a plate rheometer or another type of bulk rheometer in which a stress is applied to the biofilm and the viscous and elastic response are measured. The problem with this method is that it is difficult to study the effect of the conditions in a realistic biofouling experiment as the biofilm must be either grown on top the rheology plates or scraped off a surface and put onto the plate. Probably this affects the properties of the biofilm. So a better non-invasive measurement method is needed to study the biofilm. [4]

## 1.2 Optical Method

The method called Optical Coherence Tomography (OCT) uses the principle of light scattering and can image for example tissue or retina samples with a thickness of about $1\,\mathrm{mm}$. Recently this method has been used to study the growth of a biofilm and simultaneously the velocity profile inside a micro channel by using nanoparticles[2] This method could, in principle, also measure the viscosity and velocity profile inside a microchannel but only limited research has been done on this with a water flow.[5]. So before it can be successfully applied to growing biofilm systems, first it must be is studied in relative simple systems. In this Thesis, water solutions with a model compound called xanthan gum is used, because xanthan gum can sometimes also be found in biofilms.

Xanthan gum is an anionic polysacharide that is excreted by the bacteria *X. Campestris* with a backbone of glucose and negatively charged side groups, that are created in the presence of acids.It is well known for its thickening effects when added to water, even in very small amounts.[6]

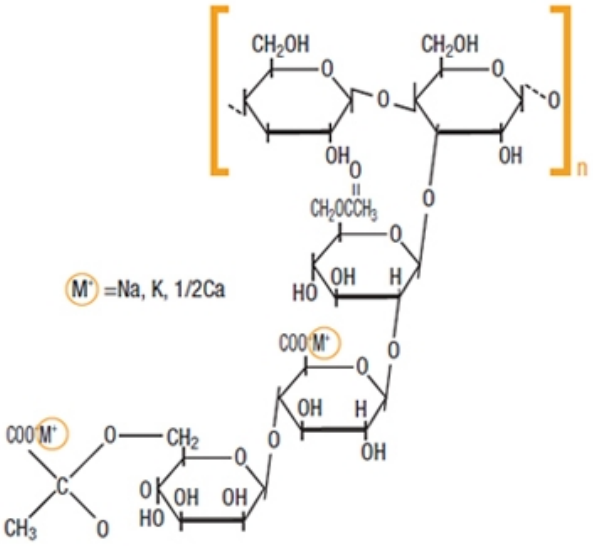


Figure 1.2: *The molecular structure of Xanthan gum . Source:[7]*

The main research question in this report is: Is it possible to measure the viscosity and velocity profile of polymeric solutions in a microchannel with Optical Coherence Tomography? In order to answer this question, xanthan gum-water solutions with different concentrations are probed by 2 different sizes of nanoparticles and the xanthan gum-water solutions are pumped through the microchannel at different flow rates.

This Bachelor Assignment will have the following structure: In chapter 2 some theoretical background information is given about the OCT device, The Brownian motion of particles and about the viscosity of fluids. This is followed by the experimental procedure that was used in chapter 3. The results of the experiments are presented in chapter 4, which is followed by a discussion in chapter 5. In chapter 6, the conclusion and recommendations on future research are presented.

# 2 Theoretical Background

## 2.1 Optical Coherence Tomography

In this project a relatively new method is used to characterize a fluid's velocity and the viscosity through a glass capillary simultaneously. This technique uses a infrared light laser source, with a small band of wavelengths that is split up in a reference signal and a sample signal. The reference signal travels along a fixed path into the detector and the sample signal is send to the sample. As the light hits the sample, some light is scattered and some will pass through it. The light that is reflected in the opposite direction is combined with the reference beam into a detector. This can be seen schematically in Figure 2.1a.[2]

Figure 2.1: *The OCT setup with light beams schematically drawn. Based on:[8] and an example OCT image of a biofilm on a surface.Source: [9]*

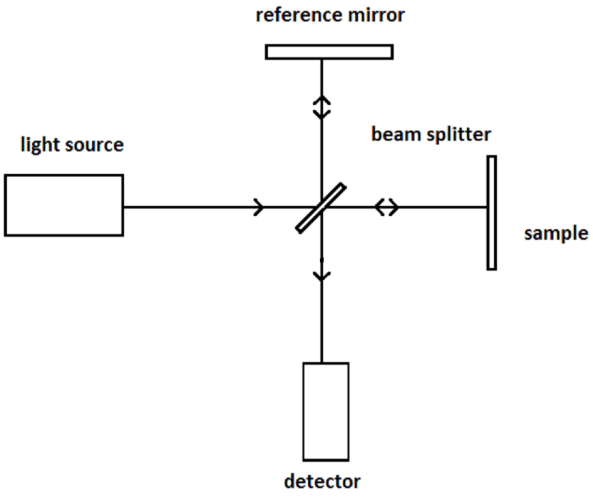


(a) *OCT setup*

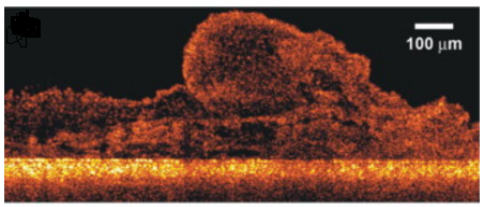


(b) *OCT image*

The light is reflected at different depths of the sample and the signal at each depth can be discriminated from each other based on the difference in the path length of the reference signal and the scattered light. As light that travels over a certain different length, it has a different

phase when it comes into the detector. A combination of both signals leads to a interfered light signal, which is a summation of both light signals. As this is done for a range of wavelengths that are emitted by the laser, this leads to a specific interference pattern of constructively and destructively interfered light of all the wavelengths for a specific difference in path length. In this way the signal is can be related to a certain depth in the sample. The OCT device processes the intensity of the reflected light into an image of the sample. Finally this results into an image, an example of an OCT image from a biofilm can be seen in Figure 2.1b[10]

In order to get a backscattering from a fluid in a capillary, nanoparticles must be used, because pure liquids do not scatter light in the bulk. This can be explained by interference of light. Light is destructively interfered when the phase difference is half of the wavelength of the light. Which is also explained by the equation:

$$d = \frac{\lambda}{2sin(\theta)} \tag{2.1}$$

In which $d$ is the distance between scattering molecules, $\lambda$ is the wavelength and $\theta$ is the scattering angle. In a bulk of a liquid there are very much molecules so there is always an molecule such spaced that every for scattering angle the light waves are canceled out, except for the propagating direction. It has been found that by adding nanoparticles to a fluid light scattering does occur. [11]

## 2.2 Brownian Motion

Small molecules, such as water molecules, have a large kinetic energy at temperatures above the absolute zero and move very fast at an atomic level, when atoms collide they affect each other, but it has been found that these collisions also affect small particles up to the micrometer scale. This phenomena is commonly known as Brownian motion.Brownian motion of nanoparticles in a solution is a random motion, but it has been found that the diffusion of such particles can be calculated. The diffusion coefficient of a nanoparticle is given by the Stokes-Einstein equation:

$$D = \frac{k_b T}{6\pi\eta r} \tag{2.2}$$

in which $k_b$ is Boltzmann's constant, $T$ is temperature in Kelvin, $\eta$ is the bulk viscosity of the solution and $r$ is the radius of the particle.[12]

However this equation gives only a correct relation between the bulk viscosity and the diffusion coefficient when the particles can move unhindered through the medium, which is not the case for particles in for example a polymer solution in which the particles will be trapped by the entanglements.

Polymers chain segments can move almost freely in a solvent, but when a particle is near the polymer, it can move in less directions which leads to a loss in configuration entropy. As a system always want to go to maximum entropy, which means that the polymers are barely present in the volume near the particles, see Figure 2.2a. So the particles have more interaction with the solvent than with the polymer and the measured diffusion coefficient of the particles is far higher than expected from the bulk viscosity of polymer solutions. This effect depends on the concentration of polymer in solution, because at a higher polymer concentration, the polymer can more difficult avoid the particles and the probed viscosity becomes more similar to the bulk viscosity. This trend can be seen in Figure 2.2b. [13, 14]

Figure 2.2: *A schematic figure of the nanoparticle depletion layer in a polymer solution and an example trend of the Stokes-Einstein viscosity with respect to the viscosity of the solvent as function of the polymer concentration, in which $\eta$ is the Stokes-Einstein viscosity and $\eta_s$ the solvent viscosity Source:[13]*

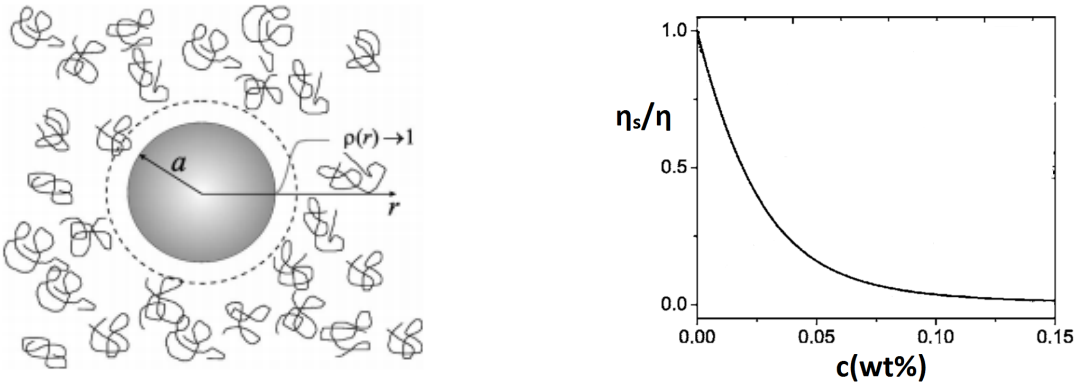


(a) *the nanoparticle depletion layer in a polymer solution*

(b) *depletion layer effect on viscosity as function of the polymer concentration*

So it is expected that the Stokes-Einstein equation will not give a representative viscosity for polymer solutions and this will probably also be the case for biofilms, because of the depletion layer theory and the assumption that the particles are not hindered by the solution. The viscosity can also be determined optically with another method which is called microrheology, which is based on the Generalised Stokes-Einstein equation. The diffusion coeffient of particles in a polymer solution depends on the time that the particles are observed. At a short timescale the particles are hindered by the entanglements of the polymer, which means that the particles move slowly, but as the particles are followed for a longer time, the entanglements of the polymers chain segments show relaxation and the particles can escape from the polymer network, which means can move more freely through the solution. Between these timescales there is an elastic plateau in which the particles are completely surrounded by polymer chains and the particles remain almost stationary.With this method the Mean Square Displacement (MSD) over time is obtained, which can be transformed into a frequency dependent viscosity from the viscoelastic parameters. [15]

This method was originally described for a Dynamic Light Scattering device in [16], which is a device similar to the OCT, except for that the scattering cannot be discriminated from each depth but measures the average scattering of the complete sample. The microrheology method is explained more extensively in Appendix B. it was adapted slightly from [16] to suit for the OCT data.

## 2.3 Viscosity & Shear Stress

Shear stress is a stress that is applied parallel to the surface of a substance. A shear stress applied to a solid causes an elastic deformation, that vanishes when the shear stress is removed. When a shear stress is applied to a fluid, a layer of fluid to which the stress is applied begins to move with a constant velocity. This layer again applies a shear stress to the fluid under it, which also moves with a different constant velocity. This process causes a linear velocity profile, which can be seen in Figure 2.3a. The exact profile depends on how well the momentum is transfered from one fluid layer to the other. A quantity that determines this is the viscosity of the fluid.[17]

Figure 2.3: *A schematic figure showing the linear velocity profile in of fluid that arises when a shear stress is applied to a fluid with the upper plate and a parabolic velocity profile of a pressure driven, laminar flow.Source:[17]*

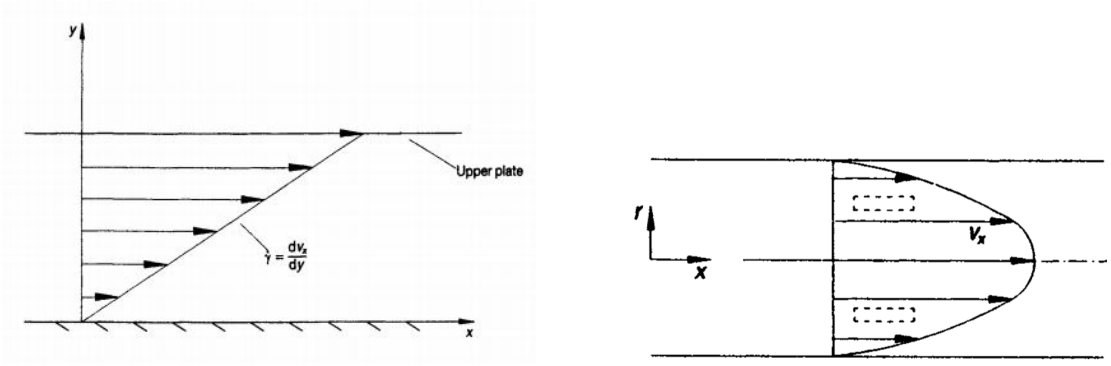


(a) *linear velocity profile* (b) *parabolic velocity profile*

The shear stress on a fluid layer is given by the following equation:

$$\sigma = \eta \frac{dv_x}{dy} \tag{2.3}$$

In which $\sigma$ is the shear stress, $\eta$ the dynamic viscosity and $\frac{dv_x}{dy}$ the velocity gradient, which is often called the shear rate. The viscosity can be seen as a resistance of the fluid to flow as a higher shear stress must be applied to a more viscous fluid to obtain the same velocity profile.[17]

A Newtonian fluid flow in a channel, driven by a pressure drop, in the laminar regime flows in a parabolic velocity profile with the highest velocity in the middle of the channel and no flow near the walls under the assumption of the no-slip condition, see Figure 2.3b. In this situation it can be derived from Equation 2.3 that the highest shear stress is applied to the fluid near the walls and almost no shear stress is applied in the middle of the channel, as the velocity gradient is maximal near the wall zero in the middle respectively. [17]

The viscosity of a fluid is for common fluids such as water or air only dependents on the temperature and pressure, such fluids are commonly known as Newtonian fluids. There is also a large group of fluids that has a viscosity that is besides a function of temperature also a function of the shear rate.These fluids are all known as Non-Newtonian fluids. The viscosity in this case is known as an apparent viscosity. For this type of fluids it is not sufficient to measure only at one specific shear stress, but it needs to be measured over a range of shear rates to obtain the Non-Newtonian relation. Xanthan gum-water solutions are known as shear thinning as well as viscoelastic fluids. [18]

### 2.3.1 Shear thinning

When the apparent viscosity drops with an increase in shear rate, the fluid's behavior is called shear thinning or pseudo plasticity. This occurs for example in polymer solutions and in dispersed particle solutions. These fluid systems are very disorganized and the different polymer chains are very entangled. As the shear rate increases, the polymer chains start to uncoil and stretch, in order to align themselves with the flow, which leads to a lowering in

viscosity. This process requires a certain amount of force in order to begin to untangle. So at low shear rates the polymer does not untangle and this leads to an apparent Newtonian viscosity, this is followed by a decreasing viscosity. As the shear rate becomes so high that all chains are already aligned, the viscosity becomes Newtonian.[18]

The viscosity can be described by different models in shear thinning liquids. For the decreasing viscosity region the fluid can be described by the Power law:

$$\eta = K(\frac{dv_x}{dy})^n \tag{2.4}$$

In which $K$ and $n$ are fitting parameters. For a shear thinning fluid $n$ has a value below between one and zero.

The parabolic velocity profile in a channel is only observed for a Newtonian fluid, because the shear stresses in a shear thinning fluid influence the viscosity and this affects also the velocity profile the profile into a flattened parabolic shape. The Power Law model is used to derive a velocity profile for a cylindrical channel [19]:

$$v_x = R\Big(-\frac{R}{2K}\frac{dP}{dx}\Big)^{\frac{1}{n}}\Big[\frac{1}{1/n+1}\Big(1-(\frac{r}{R})^{1/n+1}\Big)\Big] \tag{2.5}$$

In which $R$ is the radius of the channel, $r$ is the radial position in the channel and $\frac{dP}{dx}$ is the axial pressure gradient in the channel.

The Power law only takes the 'shear thinning region' into account, however in polymer solutions first a Newtonian plateau is passed in which the chain segments begin to untangle and at the end there is another Newtonian plateau. A model that takes into account all these viscosity regions of a polymer solution is the Carreau model:

$$\eta = \eta_\infty + (\eta_0 - \eta_\infty)\Big(1+\big(\tau\frac{dv_x}{dr}\big)^2\Big)^{\frac{n-1}{2}} \tag{2.6}$$

In which $\eta_\infty$ is the Newtonian viscosity at a high shear rate, $\eta_0$ zero shear viscosity, $\tau$ is another emperical fitting parameter for the equation. The data specifically for the experimentally used xanthan gum concentration can be found in Table 2.1 and Figure 2.4

Table 2.1: *Fitted parameters for the Power law and the Carreau equation for different xanthan gum-water solutions. Source:[19]*

| concentration (wt%) | $K$ (Pa s) | $\tau$ (s) | $n$ (-) |
|---|---|---|---|
| 0.05 | 0.0890 | 5 | 0.563 |
| 0.2 | 2.05 | 21.2 | 0.406 |

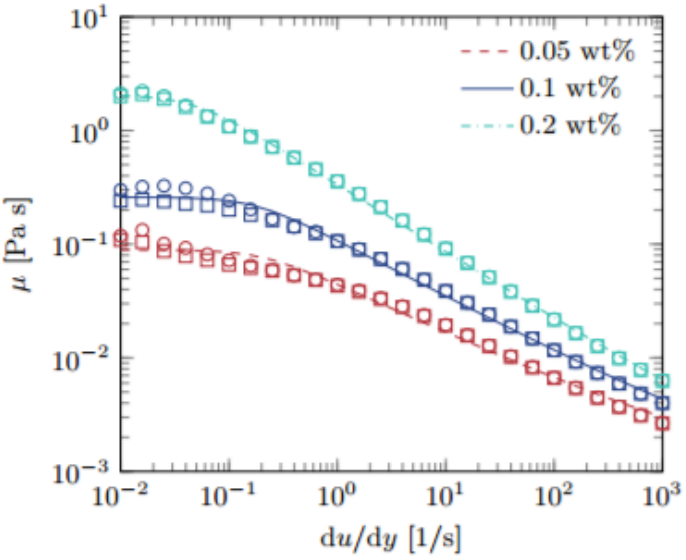


Figure 2.4: *The viscosity of Xanthan gum-water solutions as function of the shear rate. Source:[19]*

### 2.3.2 Viscoelasticity

Polymers or solutions of polymers have the characteristics solids and fluids. This means such substances behave elastically and viscous. This results in the partial recovery to the original shape when a stress on such a fluid is removed.

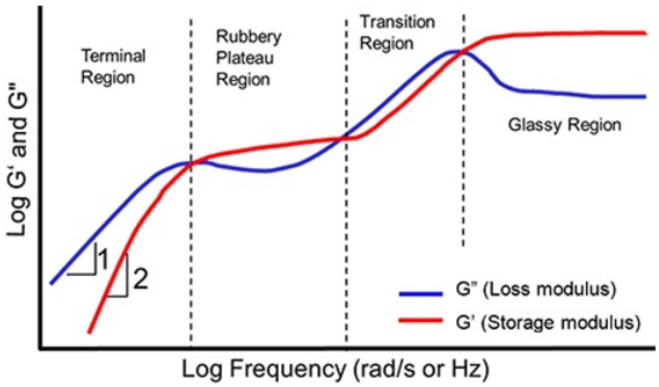


Figure 2.5: *The typical viscoelastic regimes of a polymer solution . Source:[20]*

Often viscoelastic polymers are characterized by oscillatory measurements in which the stress is periodically varied with a certain angular frequency. From these measurements a loss modulus $G''$ and a storage modulus $G'$ can be obtained, which tells something about the viscous component and elastic component of the respectively. The viscosity, which is often called the complex dynamic viscosity of an viscoelastic fluid depends both on the elastic and

viscous contribution of the moduli and is given by:

$$\eta^* = \sqrt[2]{\frac{G'^2 + G''^2}{\omega^2}} \tag{2.7}$$

in which $\omega$ is the applied angular frequency.

When a stress is applied on a polymer, first it behaves elastic and as the stress is applied longer it will become more viscous. The value of the moduli tells something about the how viscous or elastic the sample is at a specific frequency. For example at low frequencies, which corresponds to a stress applied for a long time, the polymer solution is very viscous, as can be seen in the moduli in the viscous region in Figure 2.5, which are the typical regimes for a viscoelastic polymer solution.[21]

## 2.4 OCT Data Analysis

The data from the OCT is the backscattered intensity of light in the depth and in time. This light is fluctuating over time as it is backscattered by many quickly moving nanoparticles in the light beam, it is therefore impossible to obtain information about the motion of a single particles, because this signal is an average of all positions of the particles. To find a relationship in time at a specific depth a method commonly known as autocorrelation is used. This method multiplies the fluctuating signal measured in time with the same signal and this second signal is shifted a bit forward in time. The signal is correlated to the signal with a small time-shift because the particles move by diffusion or by the velocity of the fluid, which scatters the light slightly different . However as the time-shift gets larger the original particles move through the beam until they are no longer inside the light and no correlation can be found between the original signal and the shifted signal. This results in a autocorrelated curve with a decay in the correlation as the time-shift becomes larger. The autocorrelation function is often normalized between zero and one, which mean there is no correlation or the signal is exactly the same respectively.[22]

It has been found that for a OCT signal in which a fluid flows through a capillary the following equation can be used to predict the diffusion coefficient and velocity from the normalized autocorrelated data[5]

$$g(\tau) = e^{-2Dq^2\tau} e^{-2(v_x\tau/w_0)^2} \tag{2.8}$$

in which $g$ is the autocorrelated intensity, $\tau$ the time-shift of the second signal, $D$ the diffusion coefficient, $v_x$ the velocity of the fluid in the direction perpendicular to the light beam. The Gausian beam waist is given by $w_0$, which is the radius of the light beam at its focus point . The $q$ is the scattering vector, this is a correction for the angle at which the scattered light is detected. The scattering vector is given which is given by:

$$q = \frac{4\pi n}{\lambda} sin(\theta/2) \tag{2.9}$$

In which $n$ is the refractive index of light in water, which has a value of 1.33 and $\theta$ is the angle at which the scattered light is detected, which is in the case of OCT always $180°$.

This two parameter fit equation can be understood quite intuitively, because as the particles diffuse faster or have a larger velocity the particles move faster through the light beam and

a correlation can be found over a shorter time-shift or in other words the the autocorrelation function decays faster.

It has been found previously in [5] that the diffusion coefficient by using only the first term or the velocity by filling in the diffusion coefficient with a fixed value can be fitted very accurately. However when a 2 parameter fit is used, the accuracy depends on the decay contribution of both parameters, which can be represented by the decay time constants of the diffusion and the velocity. The decay time constants are given by:

$$\tau_D = (2Dq^2)^{-1} \tag{2.10}$$

$$\tau_{vx} = (\sqrt[2]{2}v_x/w_0)^{-1} \tag{2.11}$$

When one of the decay time constants is lower than the other the lowest dominates in the fit. When both time constants are comparable the maximum error was approximately 10% for a water flow with particles in both the velocity and viscosity, which can be seen in Figure 2.6b.[5]

Figure 2.6: *a).The cross-sectional of the capillary indicating the scanning position of the OCT and the approximate position of 2 pixels. b). The relative error in the OCT 2 parameter fit, in which the dotted line represents the point where both decay time constants are equal.Source:[5]*

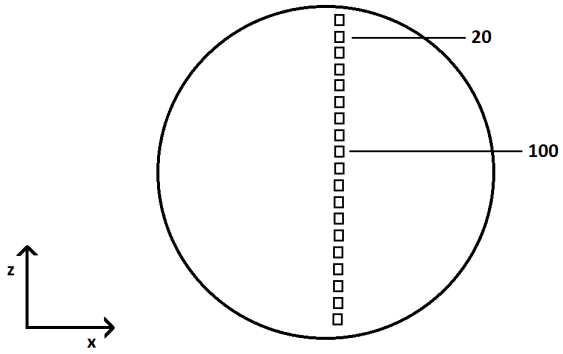


(a) *OCT scan in a capillary*

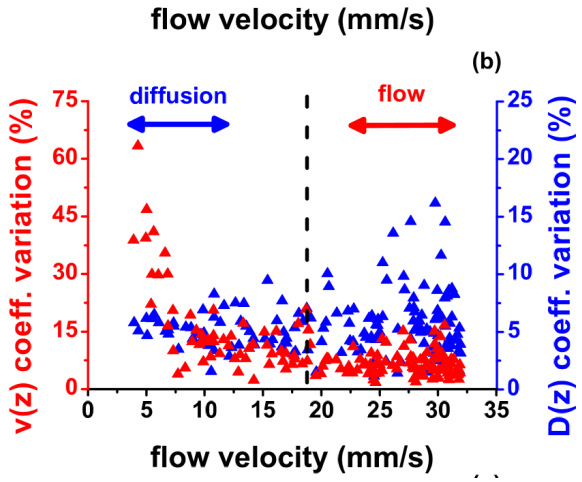


(b) *relative error in the OCT 2 parameter fit*

# 3 Experimental Procedure

## 3.1 Sample Preparation

In order to assess the capabilities of the OCT, flow and diffusion experiments were performed with water and xanthan gum-water solutions with the concentrations 0.05wt% ,0.2wt% and 0.5wt%. The water-particle solutions were prepared by dispersing $0.5\,\mathrm{mL}$ of $100\,\mathrm{nm}$ or $500\,\mathrm{nm}$ polystyrene particles with a Finn pipette into $9.5\,\mathrm{mL}$ demi-water. To prevent large aggregates, that could have formed during the storage of the nanoparticles, to be present during the measurements, the solution was put into an ultrasonic bath at room temperature for 10 minutes before every measurement. The xanthan gum-water solutions were prepared by weighing the the correct amount of xanthan gum powder with a microbalance for $30\,\mathrm{mL}$ of demi-water. The xanthan gum was purchased from Sigma-Aldrich. The next step was to dissolve the xanthan gum into water by heating demi-water to about $40\,^{\circ}\mathrm{C}$ in a $50\,\mathrm{mL}$ beaker, which was vigorously stirred with a magnetic stirrer bar.The powder was added in small amounts to prevent the formation of lumps of powder into the mixture.The nanoparticle suspension was added in the same way as the water solutions. The xanthan gum solutions were stored into the fridge to prevent biological deterioration of the xanthan gum.

## 3.2 Pump Calibration

The PHD Ultra commercial syringe pump from Harvard Apparatus was calibrated with water by weighing the amount of water that is pumped out of the syringe in one minute with a micro balance. This was done for flow rates between 5 and $25\,\mathrm{mL\,h^{-1}}$ and this was repeated up to 4 times. From this the true flow rate of the pump was determined.

## 3.3 OCT Setup

The commercial Spectral Domain OCT device from Thorlabs had a light source with a central wavelength of $930\,\mathrm{nm}$ and a bandwidth of $93\,\mathrm{nm}$. The Gaussian beam waist is $3.925\,\mu\mathrm{m}$ wide. The measurements were done with a glass capillary, which has a diameter of $0.58\,\mathrm{mm}$ and the solutions were pumped into the capillary with a syringe pump equipped with a $10\,\mathrm{mL}$ syringe from Terumo. The syringe was connected to the capillary with plastic tubing and a valve before the capillary to ensure that there is absolutely no flow when the valve is closed. This was needed for the no-flow measurements. In order to get the best backscattering signal, the light beam was focused as close to the middle of the channel as possible. Completely in the middle was impossible because at that point the glass wall reflected a lot of light, which makes the measurement unreliable.

The scanning rate at which the measurements were performed in time was primarily $10\,\mathrm{kHz}$. However for a flow-rate of $20\,\mathrm{mL\,h^{-1}}$ this was not possible at this scanning rate, because the

particles travel over a too large distance between measurements and no accurate correlation in time can be made. Therefore in these measurements a scanning rate of $30\,\mathrm{kHz}$ was used. Each measurement consisted of 10000 scans in time and this was repeated 3 times. The average result was processed to calculate the autocorrelation of the signal at about 300 volume pixels over the depth of the capilary . This autocorrelation was then fitted to Equation 2.8 or the viscoelastic parameters were calculated based on the average autocorrelation from each depth until the noise in the signal in the autocorrelation became dominant . The fitting procedure was done in MATLAB and the used fitting procedure is called nonlinear least squares fitting.

It was found that the setup is very susceptible to external vibrations, to reduce the vibrational effects on the light scattering data the capillary was mounted on clips.

For the flow measurements, the fluid was pumped at a fixed flow rate through the complete setup for a while before the actual measurement was done to be sure that the flow rate was constant and the velocity profile was steady-state. After each set of measurements with a fluid the system was cleaned completely with demi-water, before inserting a different particle solution in the syringe.

# 4 Results

## 4.1 Raw Data

In order to asses how well the autocorrelation fit works, first the quality of the raw autocorrelated data must be assessed. For clarity of the data, only 2 volume pixels at 2 different depths have been chosen from the beginning of the capillary (pixel 20) and in the middle of the channel (pixel 100), see figure Figure 2.6a. In Figure 4.1a can be seen that the autocorrelated data of the no-flow experiments with nanoparticles of $100\,\mathrm{nm}$ are in line with the expected trends as the more viscous xanthan solutions have a lower diffusion coefficient and this means it should decay slower according to Equation 2.8. Furthermore it can be seen that the signal for the most of the solutions is nearly independent of the depth. So it should be possible to obtain results for these probes.

However for the $500\,\mathrm{nm}$ probes it can be seen in Figure 4.1b that the obtained viscosity in this case can never be accurate as the decay in the graph is very little decay and in the beginning the autocorrelation at pixel 20 is drops far faster than the exponential decay. Furthermore, the decay depends much on the depth pixel at which the measurement was taken. So the quality of the autocorrelation is too bad to do a reliable fit with and it is therefore expected that the $500\,\mathrm{nm}$ polystyrene nanoparticles cannot be used to find the viscosity of the solutions.

Because of this finding the following results of the experiments are only presented for the $100\,\mathrm{nm}$ size particles.

Figure 4.1: *The raw autocorrelation data of the different particles sizes for the different xanthan gum-water solutions for the no flow measurements taken at different depth pixels.The first data point, which has a value of 1, was omitted for clarity.*

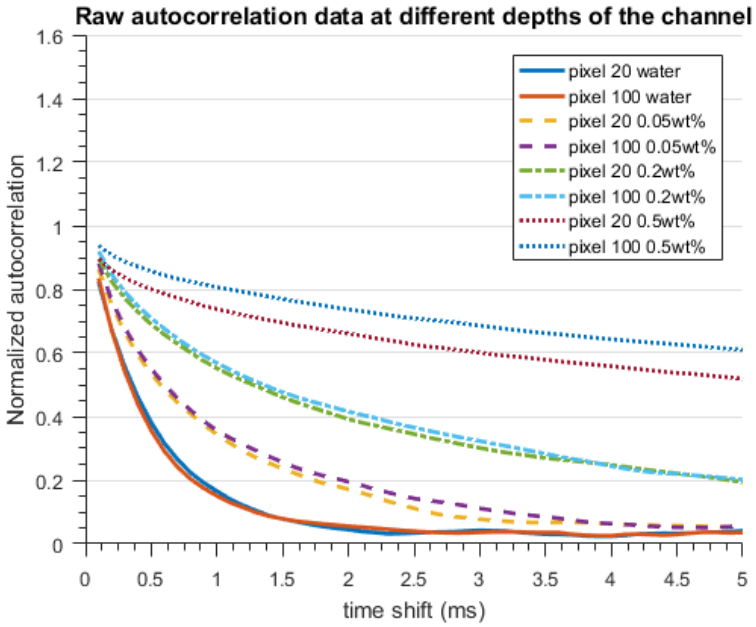


(a) *100 nm particles.*

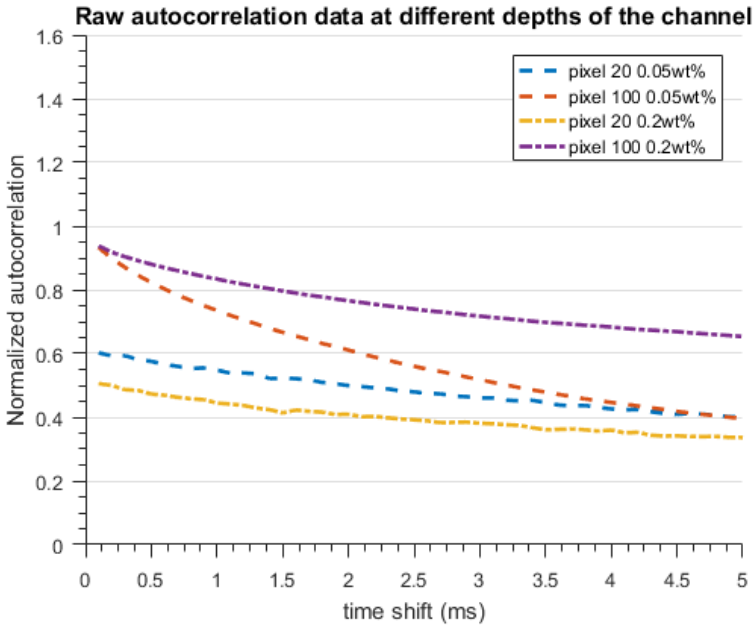


(b) *500 nm particles*

## 4.2 No-flow experiments

In this section the 2 previously mentioned models will be tested on the same raw data for the all the made water and xanthan particle solutions.

### 4.2.1 Stokes-Einstein Equation

To measure the viscosity with the Stokes-Einstein equation only the diffusion term was used from Equation 2.8, because there is obviously no flow component. The viscosity calculated with the Stokes-Einstein equation from the no-flow measurements is as expected only in agreement with the water-particle solution. It can be seen that for the xanthan solutions the viscosity is completely not in line with the bulk viscosity of the solution and the relative change in viscosity with increasing concentration is also very different from the bulk viscosity. However, it can be seen that the Stokes-Einstein viscosity increases exponentially as the concentration increases as could be seen in Figure 2.2b. So the depletion layer theory seems to be a good explanation for this effect.

Table 4.1: *The measured viscosity obtained from no-flow measurements and the bulk viscosity measured with obtained from: [19]*

| concentration (wt%) | $\eta_{measured}$ (mPa) | $\eta_{bulk}$ (mPa) |
|---|---|---|
| 0 | 0.98±0.06 | 0.93 |
| 0.05 | 2.9±0.2 | 89 |
| 0.2 | 7.7±1 | 2005 |
| 0.5 | 33±10 | - |

### 4.2.2 Microrheology

The complex dynamic viscosity is usually measured in a rheometer that applies shear stress with a certain angular frequency. In order to asses how well this is measured with the the microrheology it is compared to the mechanical rheology data of xanthan gum.

Because of the fact that the Carreau model is accurate in all viscosity regimes this is chosen as a comparison for the microrheology data. As can be seen in Figure 4.2 the trend in both viscosities is quite similar and surprisingly the difference in viscosity of the xanthan solutions calculated with the microrheology model is substantial compared to the results of the Stokes-Einstein equation, although the same data is used in both methods. As can be seen in Figure 4.3b the viscosity is also in this case not completely flat and the value is about ten times too low. However the deviation from the completely flat profile is far smaller than the differences in complex viscosity of the xanthan gum solutions. By comparing the Careau visosity for the xanthan gum solutions with the calculated viscosity it seems like the complex dynamic viscosity is also about ten times too low. So it is questionable whether this is a good tool to get the quantitative value of the viscosity, but it is certainly possible to get the trend from the data.

In principle it is also possible to in which viscoelastic regime the measurement is done from the viscoelastic storage and loss moduli. The graphs for the moduli of the xanthan gum solutions are represented in Figure 4.2 and Figure 4.3. From this it could be concluded that the measurements were done in the transition region to the glassy region. However because the viscosity does not exactly match the comparison data and there is only one regime present in the graphs, this is not hard evidence for this observation. It can be concluded that the elastic contribution to the velocity is probably the reason for the increase in viscosity as the loss modulus stays aproximately the same while the storage modulus increases, with increase in concentration of xanthan gum, see Figure A.4 .

Figure 4.2: *The calculated complex dynamic viscosity and Carreau viscosity for 0.05 and 0.2wt% xanthan gum-water solutions*

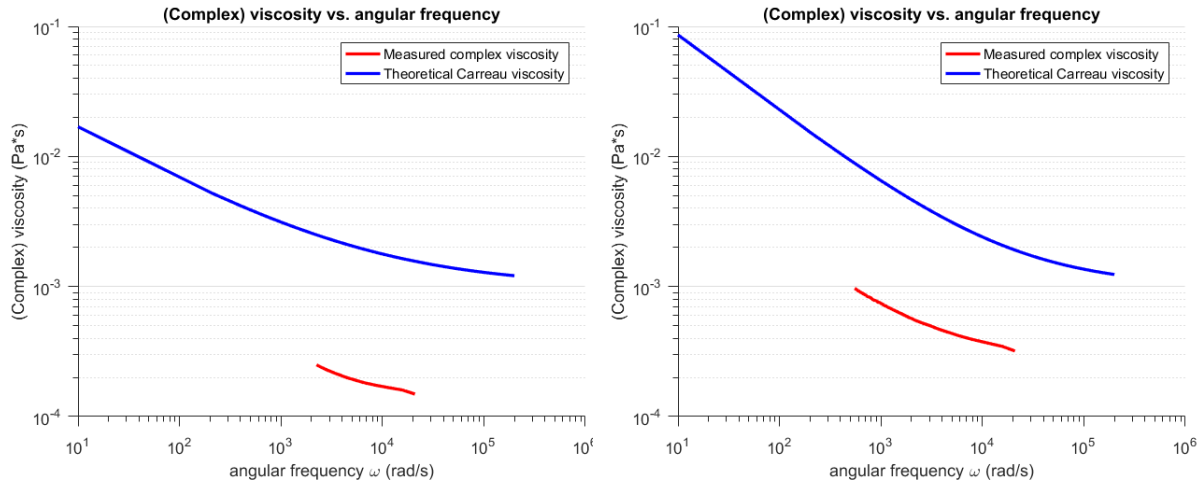


(a) *0.05wt% xanthan gum* (b) *0.2wt% xanthan gum*

Figure 4.3: *The calculated complex viscosity for 0.5wt% xanthan gum-water solution and water*

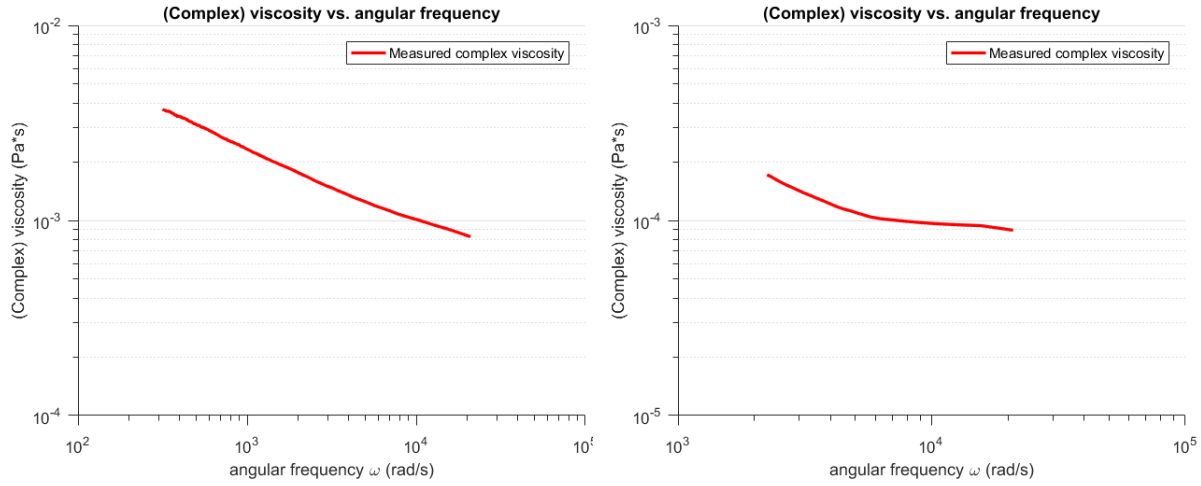


(a) *0.5wt% xanthan gum* (b) *water*

## 4.3 Characterization of the velocity profile

In order to asses how accurate the velocity can be calculated based on the correlation fit, first it must be measured how well the set flow rate matches the actual flow rate. This has been done only for the water-particle solutions only. As can be seen in Table A.1 in Appendix A the pump has approximately an error of $1\,\mathrm{mL\,h^{-1}}$ over the measured range except for the highest flow rate.

In Table 4.2 it can be seen that the maximum velocity for water fitted from the autocorrelation is very comparable to the maximum velocity that was based on the flow rate of the pump. For a Newtonian fluid it is commonly known that the maximum velocity is two times the average

Table 4.2: *The maximal velocity of the water measured with the OCT and calculated based on the flow rate of the pump for different flow rates*

| flow rate (ml/h) | $v_{max,measured}$ (mm/s) | $v_{max,calculated}$ (mm/s) |
|---|---|---|
| 3 | 5±1 | 6±2 |
| 7 | 16±1 | 14±2 |
| 20* | 53±3 | 42±4 |

* The $20\,\mathrm{mL\,h^{-1}}$ measurements were performed a scanning rate of $30\,\mathrm{kHz}$

velocity and this can be calculated from the flow rate with:

$$v_{x,max} = \frac{2Q}{A} \tag{4.1}$$

In which $Q$ is the flow rate of the pump and $A$ the cross-sectional area of the capillary. It can be seen that the measured maximum velocity is in line for the lowest flow rates. Only the $20\,\mathrm{mL\,h^{-1}}$ (Figure A.2a) shows a large deviation with set flow rate, which is probably caused by the increasing inaccuracy in the set flow rate or by the quicker scanning rate that has been used for this measurement. Although the maximum velocity of $3\,\mathrm{mL\,h^{-1}}$ is in line with the flow rate, it should be noted that the data points in velocity are very broadly distributed, which can be seen in Figure A.1a, which is probably caused by the fact that the diffusion greatly influences the velocity of the particles.

Figure 4.4: *The velocity and viscosity profile measured for different xanthan gum-water solutions at a flow rate of* $7\,\mathrm{mL\,h^{-1}}$

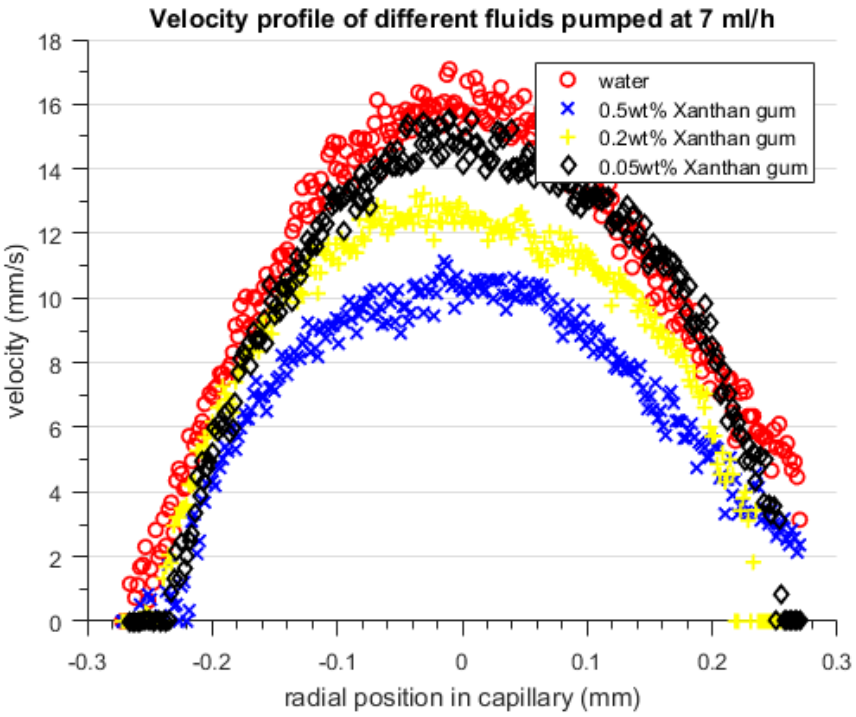


(a) *velocity profile*

.

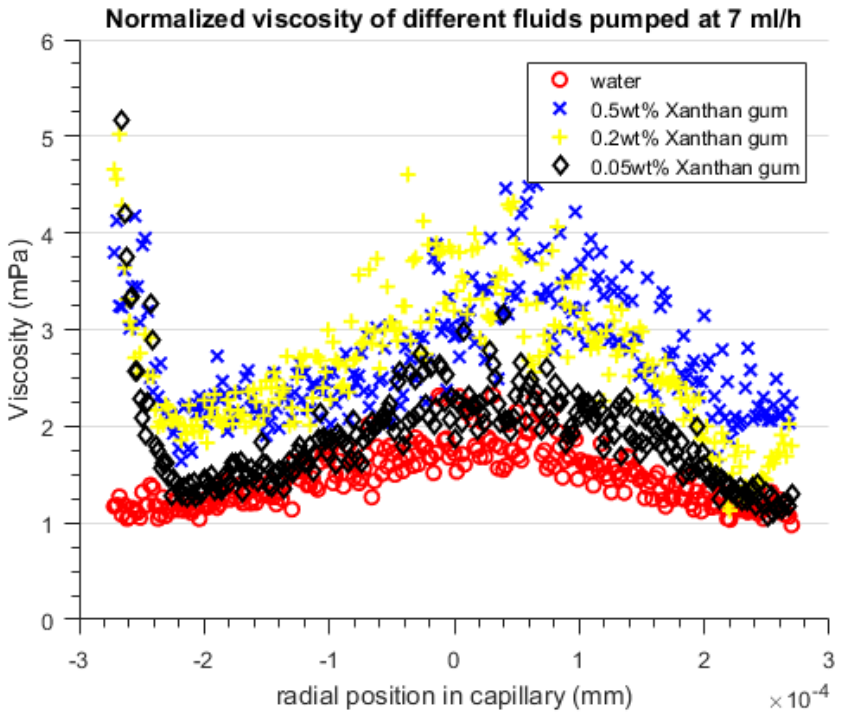


(b) *viscosity profile*

.

It is expected that for the xanthan solution measurements the should have approximately the

Table 4.3: *The fitted shear thinning parameter at different concentration of xanthan-water solutions and water at flow rates of 7 and* $20\,\mathrm{mL\,h^{-1}}$. *The fitted data was compared to measurements done with a mechanical rheometer. Obtained from:[19]*

| concentration (wt%) | $n_{fit}$ at 7 ml/h | $n_{fit}$ at 20 ml/h | $n_{theory}$ |
|---|---|---|---|
| 0 | 1.1±0.1 | 1.8±0.8 | 1 |
| 0.05 | 0.76±0.07 | 0.59±0.1 | 0.563 |
| 0.2 | 0.63±0.04 | 0.76±0.07 | 0.406 |
| 0.5 | 0.81±0.08 | 1.2±0.1 | - |

same maximum velocity as the water particle solutions, because the pump has a fixed flow rate. The shape of the velocity profile for the xanthan solutions should flatten in the middle, due to the shear thinning behaviour. However it can be seen that for all flow rates the maximum velocity drops very much as the solutions become more viscous, so this is probably not only caused by the shear thinning behaviour. The characteristic more flattened top of the parabolic profile with increasing xanthan gum concentration can be seen only clearly for the $7\,\mathrm{mL\,h^{-1}}$ velocity profile, which is depicted in Figure 4.4a.

In order to verify that the shape of the velocity profiles in the capillary are characteristic for the shear thinning fluid solutions and the Newtonian water-particle solutions, Equation 2.5 in principle could be used to fit the parameters. However in the current experimental setup it was not possible to measure the pressure drop over the capillary. Therefore the equation was simplified by dividing the maximum velocity over the velocity profile, which leads to the following theoretical equation:

The velocity profiles of 7 and $20\,\mathrm{mL\,h^{-1}}$ were chosen to fit to the equation, as it can already be seen in Figure A.1a that the spread in data in very large compared to the other flow rates. For the fit the $n$ and $R$ were chosen as fitting parameters. The $R$ was also chosen as a fitting parameter as it is hard to decide at which depth the capillary exactly starts as the scattering data near the wall is disturbed by the reflection of light from the glass wall. It can be seen in Table 4.3 that the results are quite good for water, but most of fitted shear thinning parameters the xanthan solution it can be only concluded that the shear thinning behavior of the viscosity can only be obtained qualitatively, but do not quantitatively match the data from literature. An clear example of the normalized velocity profile fit can be seen in Figure 4.3

Figure 4.5: *The normalized velocity profiles of 0.05wt% xanthan gum and water. The drawn lines are there only for comparison between a shear thinning fluid and water*

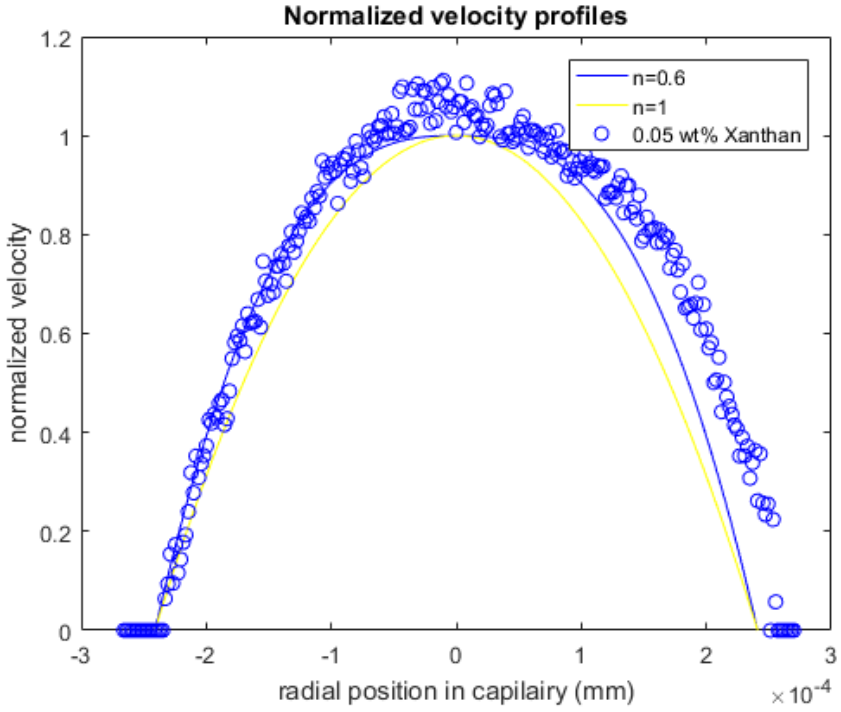


(a) *0.05wt% xanthan gum*

.

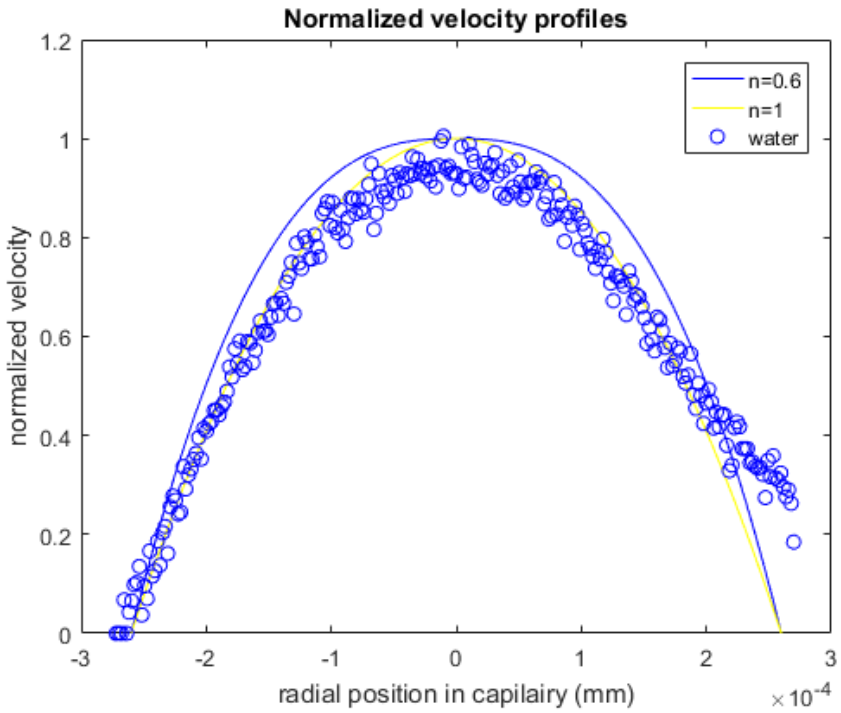


(b) *water*

.

## 4.4 Viscosity Profile

In order to derive the the viscosity from the 2 parameter fit, again the Stokes-Einstein equation was used, because microrheology is not suitable for particle solutions with a flow component, so it is primarily to see whether there are relative differences in the viscosity of the various solutions, and between the regions where much shear stress is applied on the solution and where no shear is applied to the solutions.

In the viscosity profiles of 7 and $20\,\mathrm{mL\,h^{-1}}$, which can be seen in Figure 4.4b and Figure A.3b respectively, a small increase can be seen in the middle of the channel and a decrease at the edges of the channel which is the exact profile that can be expected from a shear thinning fluid. However there are a few things that seem to be odd: Firstly the viscosity of the xanthan fluids, except for the lowest concentration, in the middle of the channel does by far not match the viscosity that was measured during the no-flow measurement though in both cases there is zero shear applied on the fluid. Secondly, it should be noted that the viscosity of water also shows a shear thinning effect, which is obviously incorrect as water is commonly known as a Newtonian fluid. To see whether the increase in the water viscosity is an error from the fit, the viscosity profile was normalized with respect to the water viscosity profile. From this new profile which can be seen in Figure 4.6, it like the same error is in the viscosity of the xanthan gum solutions, which means that that the shear thinning behaviour of the xanthan gum solutions is negligible based on the 2 parameter fit, but based on the shear rate that is applied to the fluid it should be shear thinning (see Figure 2.4. In Figure A.3a the shear thinning behaviour cannot be seen in the viscosity profile, except for the highest concentration of xanthan gum.

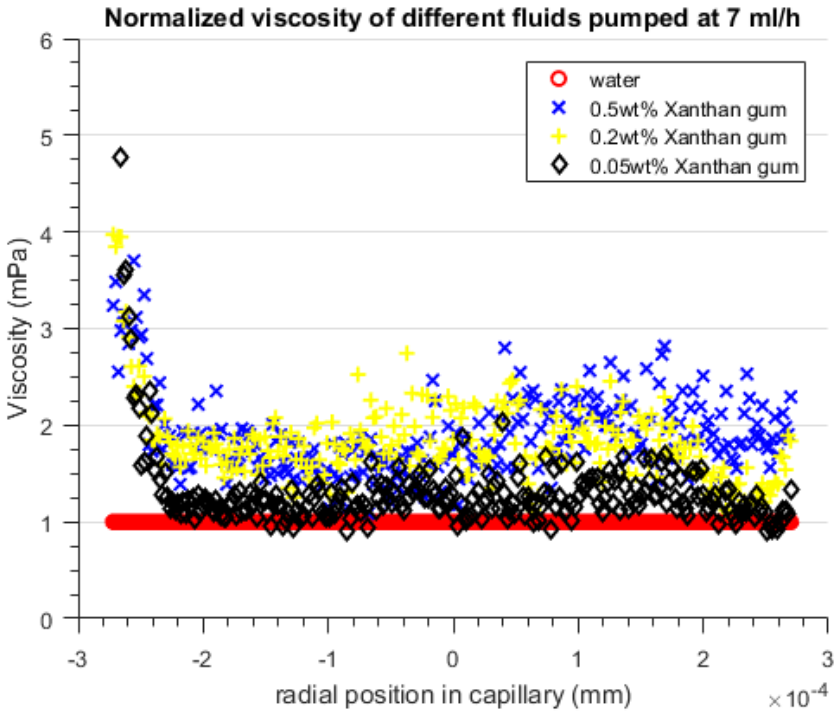


Figure 4.6: *The normalized viscosity profile measured for different xanthan-water solutions normalized over the viscosity of water*

Figure 4.7: *The relative error (95 %confidence interval) of the fit as function of the velocity* for water with a flow rate of $20\,\mathrm{mL\,h^{-1}}$

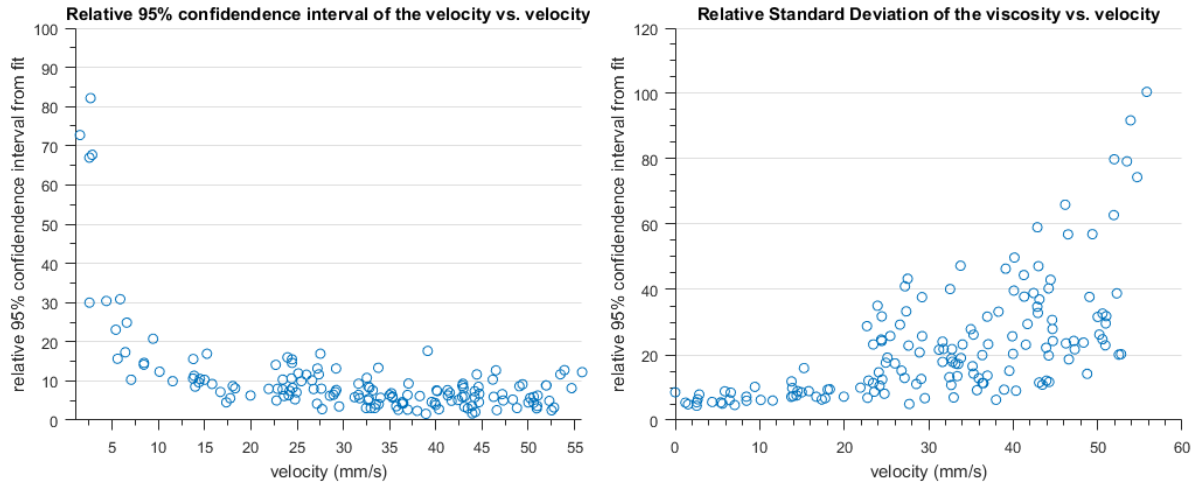


(a) *relative error in the velocity* (b) *relative error in the viscosity*

In order to asses where the viscosity of the fluid can be accurately estimated, The relative 95% confidence interval of the fit was plotted against the velocity in the channel. This relative 95% confidence interval was calculated by dividing the standard deviation from the fit by the value of the fitted viscosity or velocity. From the error it becomes clear that there is a similar trend for all measurements in the error as was earlier observed in Figure 2.6b. An example of such graphs can be seen in Figure 4.7. To see whether this error is also for the xanthan gum solutions related to the previously mentioned decay time constants, the interception point of the decay constants was obtained in depth, an example of this can be seen in Figure 4.8. This corresponds to a velocity from the velocity profile that should indicated the border between the accuracy regimes of the two parameter fit. The velocity of the relative 95% error, where the error becomes higher then 10% was then compared to the border based on the decay constants. The results for a flow rate of $7\,\mathrm{mL\,h^{-1}}$ are given in Table 4.4 and the rest of these results can be found in Appendix A.

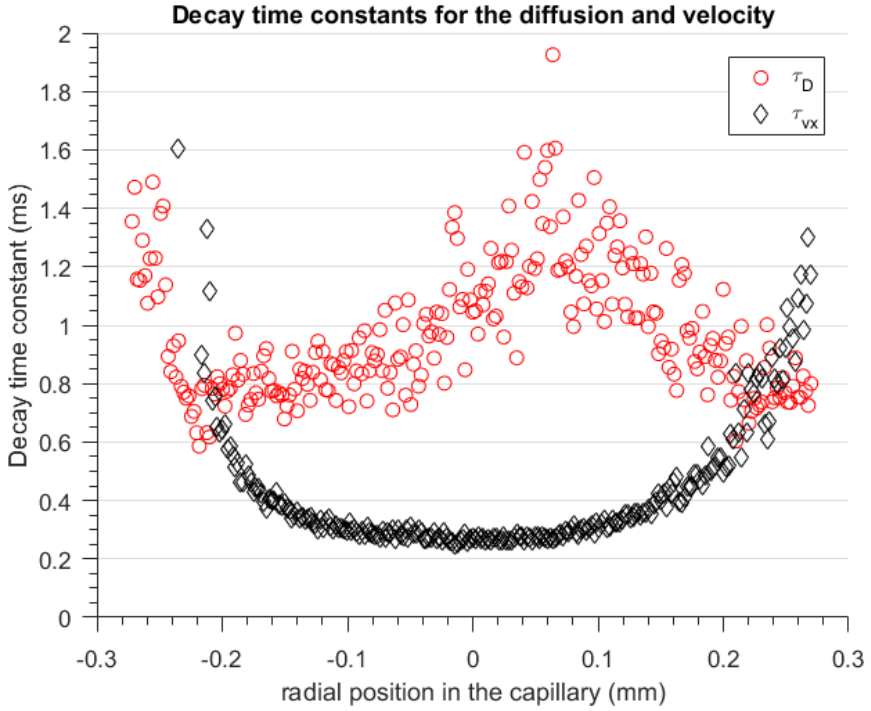


Figure 4.8: *The decay time constants for the velocity and diffusion for a xanthan gum solution of 0.5wt%*

Table 4.4: *The velocity measured for the intercept of the decay time constants and the first velocity for which the relative error in the viscosity is larger than 10 percent for a flow rate of* $7\,\mathrm{mL\,h^{-1}}$

| concentration (wt%) | $v_{x,decay}(mm/s)$ | $v_{x,95\%confidence-interval(mm/s)}$ |
|---|---|---|
| 0 | 8 | 4 |
| 0.05 | 5 | 3 |
| 0.2 | 3 | 3 |
| 0.5 | 2 | 1 |

From this it can be seen that, as was found previously, for the water particle solution the decay time constant intersection, apart from some outliers, gives a clear border between the accuracy regimes of the two parameters. The same holds true for the xanthan gum solutions, which means this finding is independent of the viscosity of a solution. In principle the decay time constants can be calculated theoretically to improve the region from which viscosity is accurately fitted, though this is very difficult for the xanthan solutions because the decay time constant is affected by the depletion layer and it depends also on the position in the capilary. It can be concluded that the error arises in the two parameter fit because the parameter with the lowest decay time constant, which means it has the slowest decay of the two parameters is dominant in the decay of the autocorrelation. It can be seen by comparing Table 4.4 with the velocity profiles and in Figure 4.8 that the accuracy of the viscosity is only high at the edges of the channel which gives only a very small region from which the viscosity can be retrieved accurately.

With this information the results from the viscosity close to the edge of the capillary of can be combined as close to the wall every flow rate causes a different shear stress on the fluid.

The shear rate was roughly estimated from the velocity profile by numerically calculations in MATLAB and using a 4th order central difference routine. From the graph in Figure 4.9 it becomes clear that in this way the shear thinning behavior graph can be made for every concentration of xanthan gum and the trend of the Careau viscosity is roughly the same as the trend in the Stokes-Einstein viscosities. Also it can be seen that as the concentration of xanthan increases the trend becomes more similar to the bulk viscosity.

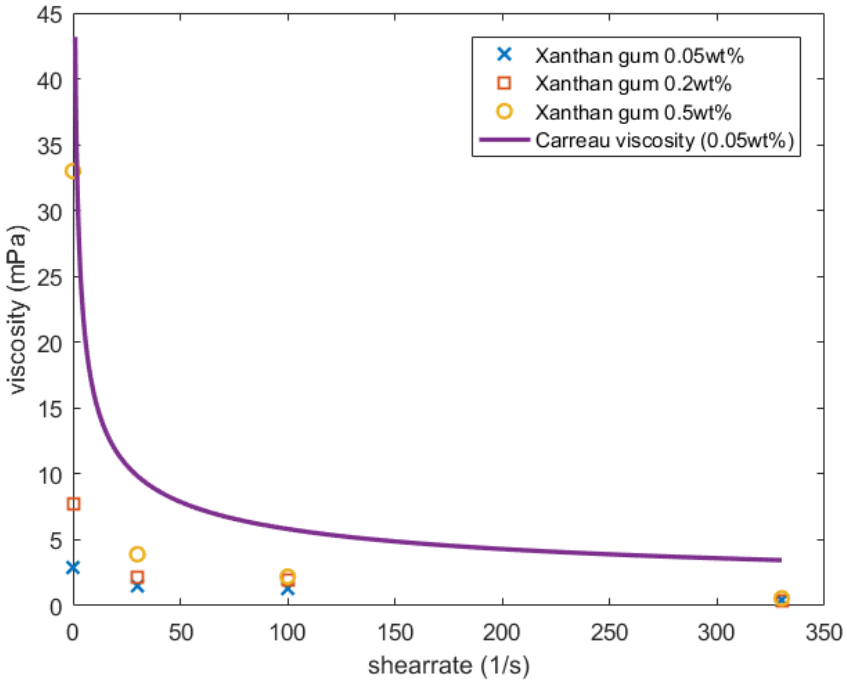


Figure 4.9: *The relative viscosity profile from all flow rates and diffusion measurements. The Careau viscosity is taken for the lowest xanthan concentration used to show the trend in the bulk viscosity*

# 5 Discussion

In chapter 4 it was found that the viscosity of water from the Stokes-Einstein equation was very different from the results from the microrheology, although it uses exactly the same raw data. It is also seen that the microrheology gives almost a fixed difference for all concentrations of xanthan gum and water, when it is compared to the mechanical rheological data. The measured velocity profiles were mostly in line with the flow rate, but the viscosity profiles from the two parameter fit are questionable based on the normalization with respect to the water viscosity and the fitting error of the viscosities. In this chapter the results will be discussed and it is tried to propose an explanation for the observed results.

The data for the behavior of the viscosity of xanthan gum that was obtained with a mechanical rheometer from the same source that was used in this Bachelor thesis. However xanthan gum is a biopolymer which makes a comparison with this data harder, because the powder might deteriorate as it is stored at room temperature and the chains might have been damaged by the temperature of $40\,^{\circ}\mathrm{C}$ that was used to dissolve it more quickly into the water. A second problem with xanthan gum is that it is very sensitive to the amount of xanthan gum that is added to the water and due to measurement errors in the weighing of the powder, this might also lead to a slightly different viscosity. The measurements were also done with xanthan without nanoparticles, but as the concentration of particles is very low it probably has a negligible effect on the viscosity.

The mechanical rheological data was measured at relative low shear rates. However the microrheology method gives information about much higher shear rates. The extrapolation the data might result in a incorrect comparison between the optical and mechanical viscosity. However based on the comparable trend between both methods, the extrapolation of the data is probably possible in this case.

Another important factor could be the actual size of the nanoparticles. A sample of the same nanoparticles have been tested with a Nanosizer from Malvern in a previous research, which resulted in Figure 5.1, in which it can be seen that the distribution in size is quite large compared to the nominal size of $100\,\mathrm{nm}$. So there is an error in the calculations of the viscosity and microrheology parameters equation as a size of $100\,\mathrm{nm}$ was assumed. However the measured data deviates so much from the expected values, especially for the Stokes-Einstein viscosities, that this cannot be caused only by a deviation in the size of the particles. The size distribution could be a reason why the measured viscosities are broadly spaced in value as the larger particles diffuse slower through the medium than the smaller ones.

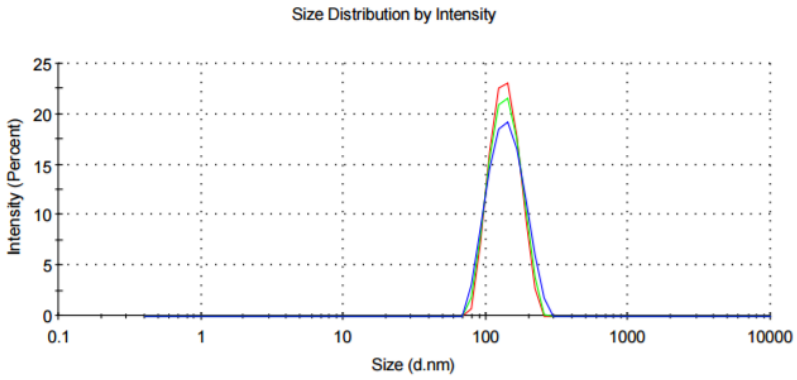


Figure 5.1: *The size distribution of the used nanoparticles with a nominal size of 100 nm.*

## 5.1 No Flow Measurements

The reason for the difference between the bulk and measured viscosity has been thought to be caused by a depletion layer around the particles. This can also be explained by the electric charge of the particles and the polymer, because they are both negatively charged, which could also result in the exclusion of the particles close to the polymer.

The deviation in the viscosity from the microrheology model can be explained by several reasons: Firstly the error might be caused because of the depletion layer or electrostatic interactions as has been the explanation for the deviation Stokes-Einstein viscosity. It might also be an yet undiscovered error inside the used MATLAB code, which is also a reasonable explanation as the difference between the Carreau equation and the viscosity seems to be a factor of 10 lower in all measurements including the water particle solution, which was accurately predicted by the Stokes-Einstein equation.The deviation can also originate from the experimental data as this method is originally used in a Dynamic Light Scattering device which uses the light scattering over a complete depth of a sample instead of the average autocorrelation from at each depth as has been done in this report. It is expected that the primary reason is in the averaging of the autocorrelation, because microrheology has been applied successfully already in DLS and the code has been checked for several times.

The curve in the viscosity of water that was obtained with microrheology can be explained by the fact that it was fairly difficult to see in the average autocorrelation where the signal to noise ratio was too bad to use this method. In the xanthan solutions this has also an effect but it cannot be seen clearly in the viscosity diagram. For the xanthan solutions this can be observed clearly in Figure A.4 as the moduli are noisy and sometimes go down, which is not in line with Figure 2.5.

## 5.2 Flow Experiments

It can be seen in the velocity profiles that the profiles are not taken from the exactly the same position inside the capillary. This is probably caused by the fact that it was hard to measure the capillary at the same spot as decoupling of the syringe, to clean the system or to fill it with a different particle solution, caused already a small displacement of the capillary. However the difference is very small so it is probably fair to compare the profiles with each other.

The unexpected drop in the maximum velocity in Figure 4.4a,Figure A.1a and Figure A.2a of the velocity profiles as the solutions have a higher xanthan concentration, might as already discussed by the flattening of the top of the profile due to shear thinning behaviour of the viscosity. However this effect seems too large to cause such a drop in maximum velocity. However no probable other reason could be thought of for this effect. It is therefore essential that the pressure drop is measured, in order to fit the complete velocity equation and the velocity profile can be verified.

The deviation in the viscosity measurements may be caused by errors in the 2 parameter fit as was stated previously due to the dominance of one of parameter's decays in the autocorrelation. However another reason could be caused by the effect of the flow on the diffusion of the particles. In a measurement with flow the particles can only have a diffuse motion in the direction perpendicular to the flow as the Brownian motion has far less effect on the movement of the particle than the velocity of the fluid. This can have an influence on the derived viscosity from the fit. Another consequence of this is that a small relative error in the fit does not guarantee that the viscosity is representative for the fluid. However due to the depletion layer around the particles this was already not possible and there is still a relative difference that can be obtained from the accurate fit position in concentration and in applied shear stress.

Another value that is important to determine the accuracy of the fit is the number of points MATLAB selects to do the fit over. As it may occur that the error for the fit is very low, but as the number of points used to fit the autocorrelation with is also low it might not be very representative for the whole autocorrelation curve. From the number of points that were used it becomes clear that with increasing velocity the number of points drop, up to 5 points at a velocity of $50\,\mathrm{mm\,s^{-1}}$ so the initial accuracy of the viscosity is still accurate because this is at a low velocity. However this makes the accuracy of the velocity in the middle of the channel questionable. This could be an explanation for the deviation in the fitted parameters of the normalized velocity profile.

The light scattering intensity might also play a role in the accuracy of the autocorrelation from the scattering, because less light reached the bottom of the channel, which is quite intuitive as the chance that light scatters increases as the light travels deeper into the capillary. The effect of the light intensity can be seen in all velocity profiles the second half of the profile shows some deviations. It was not possible to obtain the same light intensity from the complete capilary and the intensity deviated also a bit in every measurement so this could also influence the data.

# 6 Conclusion

Already from the raw data it could be seen that it is very important to use the right size of nanoparticles. It has also been found by doing the no flow measurements that the diffusivity of the particles in polymeric solutions cannot be used to measure the bulk viscosity quantitatively. Although, by using the microrheology method that is based on the generalized Stokes-Einstein equation, a viscosity with a similar trend as the viscosity, that was obtained by mechanical rheology, can be obtained. As it was observed that the difference between the bulk viscosity and the measured viscosity was in every measurement about 10 times, it can be concluded that with microrheology potentially valuable data can be obtained from polymer solutions.

For the measurements with flow it can be concluded that the velocity profile can be obtained accurately from the two parameter fit and the shear thinning behavior of the xanthan gum solutions can be obtained qualitatively from the normalized velocity profile fit.

It has been found that the bulk viscosity of a dilute polymer solution is not possible to obtain the relative viscosity profile from a single flow rate measurement with the OCT as the error in the two parameter fit is over a large part of the profile very inaccurate. It has been shown that the decay time constants are also important for estimating for which range of velocities the viscosity is still accurate in xanthan solutions and that this estimate is not only valid for water, as was shown previously in another research, which can be found in [5]

However from the combination of the reliable viscosities from various flow rates and the no-flow results with the corresponding shear rates shows that also with the Stokes-Einstein equation the relative shear thinning behavior can be observed, which has a trend that is in line with the Careau equation.

## 6.1 Recommendations

The experiments performed were as discussed in chapter 5 not perfect and in this chapter some enhancements and extension of the current experiments or setup are proposed.

The experiments can be greatly improved by measuring the actual viscosity of the solutions that were made, because a real comparison with the data from other xanthan gum solutions is not very accurate as a small deviation addition of xanthan gum or the addition of nanoparticles probably changes the viscosity significantly.

To reduce the chance to damage the xanthan gum with a higher temperature the xanthan gum can be dissolved next time only by stirring the solution vigorously over night or in the ultrasonic bath.

It has been found that the beam waist of the light has a large effect on the accuracy of the fitting of the velocity and the viscosity as this influences the decay time constant of the velocity. In the current setup it was not possible to use different beam waists. However by changing the beam waist potentially the parameters can be estimated more accurately. To obtain the most accurate result for both parameters switching between beam waists could be considered. In order to do

this a small beam waist for the estimation of the velocity and a large beam waist for the fitting of the viscosity should be used.

The particles that were used are negatively charged polystyrene nanoparticles. As discussed earlier the xanthan gum chains are also negatively charged. The effect of the charge of the particles can be tested by using a range of negative and positive charged particles of approximately the same size in xanthan gum solutions.

The frequency of the complex viscosity, that was measured with microrheology, is inversely proportional to the timeshift in the autocorrelations. The frequencies at which this was measured were quite high and are not very practical as in laminar fluid flows the shear rate is far lower. This can be enhanced by using larger particles, because the diffusion is lower and so the decay time is larger until the noise is dominant this will give information about the viscosity at lower frequencies.

The velocity profile was normalized, because the pressure drop could not be measured over the capillary within this assignment. So the use of the complete velocity profile with Equation 2.5 would give too much fitting parameters. The measurement of the pressure drop would certainly be an improvement as the parameter $K$ could also be recovered from such a fit. Furthermore can be confirmed whether the large drop of the maximum velocity is only due to the shear thinning behavior of the xanthan gum fluid.

The shear thinning behavior could be recovered from the flow experiments, but this was a very rough trend as the experiments were performed with only a few different flow rates and concentrations. To really see how well this method works a lot more flow rates and concentrations of xanthan gum could be measured.

The goal of the assignment was to asses whether it was possible to measure the viscosity and velocity profile. A next step in the application of these methods could be the measurement the viscoelastic and viscosity of a growing biofilm in a microchannel as the biofilm is a very concentrated mix of polymeric substances (EPS), there is probably a limited effect of the depletion layer on the Stokes-Einstein viscosity and microrheology could maybe be applied simultanously with the flow as deep in the biofilm there is only diffusion. A biofilm is also very heterogenous in composition so the OCT may be an essential tool to measure these properties at each depth.

In a future research the effect of the light intensity from the nanoparticles could be studied by varying the nanoparticle concentration that is used in the solutions, as it was seen that the second half of the channel gave a less accurate fit and also less light from the second half of the channel reaches the detector

By using a more monodisperse solution of nanoparticles, the diffusion of the particles is more uniform and this might also give less broadly distributed result in the viscosity profiles.

The number of points that were used in the two parameter fit dropped, at higher velocities to a minimum of 5 points, but it is unknown how many points are needed for the autocorrelation fit to give a representative result of the measured autocorrelation. Therefore an analysis should be done to verify the exact limits of the fitting procedure.

# 7 | Bibliography


[1] Thang Nguyen, Felicity A. Roddick, and Linhua Fan. Biofouling of water treatment membranes: A review of the underlying causes, monitoring techniques and control measures. *Membranes*, 2(4):804–840, 2012.

[2] Nicolás Weiss, Khalid El Tayeb El Obied, Jeroen Kalkman, Rob G.H. Lammertink, and Ton G. van Leeuwen. Measurement of biofilm growth and local hydrodynamics using optical coherence tomography. *Biomed. Opt. Express*, 7(9):3508–3518, Sep 2016.

[3] James W. Fairley. Biofilms and human infection – an introduction, 2014. `http://entkent.com/biofilms-and-infection/`.

[4] Nicole Billings, Alona Birjiniuk, Tahoura S Samad, Patrick S Doyle, and Katharina Ribbeck. Material properties of biofilms—a review of methods for understanding permeability and mechanics. *Reports on Progress in Physics*, 78(3):036601, 2015.

[5] N.M. Weiss. *The amplitude and the phase or: Measuring directional and random motion with optical coherence tomography*. PhD thesis, Amsterdam, 2016. Chapter 3.

[6] F. Garcia-Ochoa, V.E. Santos, J.A. Casas, and E. Gomez. Xanthan gum: production, recovery, and properties. *Biotechnology Advances*, 18(7):549 – 579, 2000.

[7] Cargill Incorporated. `https://www.cargill.com/food-bev/emea/hydrocolloids/xanthan-gum`. Date accessed: 28-06-2017.

[8] Photonics Media. `https://www.photonics.com/Article.aspx?AID=57706`. Date accessed: 20-6-2017.

[9] C. Dreszer, A.D. Wexler, S. Drusová, T. Overdijk, A. Zwijnenburg, H.-C. Flemming, J.C. Kruithof, and J.S. Vrouwenvelder. In-situ biofilm characterization in membrane systems using optical coherence tomography: Formation, structure, detachment and impact of flux change. *Water Research*, 67:243 – 254, 2014.

[10] A. Gh. Podoleanu. Optical coherence tomography. *Journal of Microscopy*, 247(3):209–219, 2012.

[11] Miroslaw Jonasz and Georges R. Fournier. Chapter 1 - basic principles of the interaction of light with matter. In Miroslaw Jonasz and Georges R. Fournier, editors, *Light Scattering by Particles in Water*, pages 1 – 32. Academic Press, Amsterdam, 2007.

[12] Chang Soo Kim, Wenjuan Qi, Jun Zhang, Young Jik Kwon, and Zhongping Chen. Imaging and quantifying brownian motion of micro- and nanoparticles using phase-resolved doppler variance optical coherence tomography. *Journal of Biomedical Optics*, 18(3):030504–030504, 2013.

[13] Tai-Hsi Fan, Jan K. G. Dhont, and Remco Tuinier. Motion of a sphere through a polymer solution. *Phys. Rev. E*, 75:011803, Jan 2007.

[14] Anna Ochab-Marcinek, Stefan A. Wieczorek, Natalia Ziebacz, and Robert Holyst. The effect of depletion layer on diffusion of nanoparticles in solutions of flexible and polydisperse polymers. *Soft Matter*, 8:11173–11179, 2012.

[15] T. G. Mason, K. Ganesan, J. H. van Zanten, D. Wirtz, and S. C. Kuo. Particle tracking microrheology of complex fluids. *Phys. Rev. Lett.*, 79:3282–3285, Oct 1997.

[16] Malvern Instruments Limited. An introduction to dls microrheology. `https://cdn.technologynetworks.com/TN/Resources/PDF/WP120917IntroDLSMicro.pdf`. Date Accessed: 7-6-1017.

[17] F.A. Holland and R. Bragg. 1 - fluids in motion. In F.A. Holland and R. Bragg, editors, *Fluid Flow for Chemical Engineers (Second Edition)*, pages 1 – 69. Butterworth-Heinemann, Oxford, second edition edition, 1995.

[18] C. Blom, R.J.J. Jongschaap, and J. Mellema. *Inleiding in de reologie: reometrie, dispersiereologie, polymeerreologie*. Universiteit Twente, 1986.

[19] Andries Sander Haase. *Transport near slippery interfaces*. PhD thesis, Enschede, 2016. Chapter 4.

[20] Azo Materials. `http://www.azom.com/article.aspx?ArticleID=12366`. Date accessed: 27-6-2017.

[21] P. Sunthar. *Polymer Rheology*, pages 171–191. Springer New York, New York, NY, 2010.

[22] B.J. Berne and R. Pecora. Dynamic light scattering: With applications to chemistry, biology, and physics. Dover Books on Physics Series, chapter 2. Dover Publications, 2000.

# A Additional results

## A.1 Pump Calibration

To test the accuracy in the flow that is measured in an OCT system, first the accuracy in the syringe pump was tested by pumping water with a $10\,\mathrm{mL}$ and weighing how much water is pumped in one minute.

Table A.1: Calibration data of the syringe pump

| flow rate (mL/h) | #1 (g/min) | #2 (g/min) | #3 (g/min) | #4 (g/min) | flow rate calculated (mL/h) |
|---|---|---|---|---|---|
| 5 | 0.14 | 0.097 | 0.095 | 0.096 | 6.42 |
| 10 | 0.1688 | 0.1699 | 0.1666 | 0.1680 | 10.1 |
| 15 | 0.266 | 0.264 | 0.267 | - | 15.9 |
| 20 | 0.399 | 0.349 | 0.342 | - | 21.8 |
| 25 | 0.466 | 0.438 | 0.452 | - | 27.1 |

## A.2 Velocity & Viscosity profiles

Figure A.1: The velocity & normalized viscosity profile for a flow rate of $3\,\mathrm{mL\,h^{-1}}$

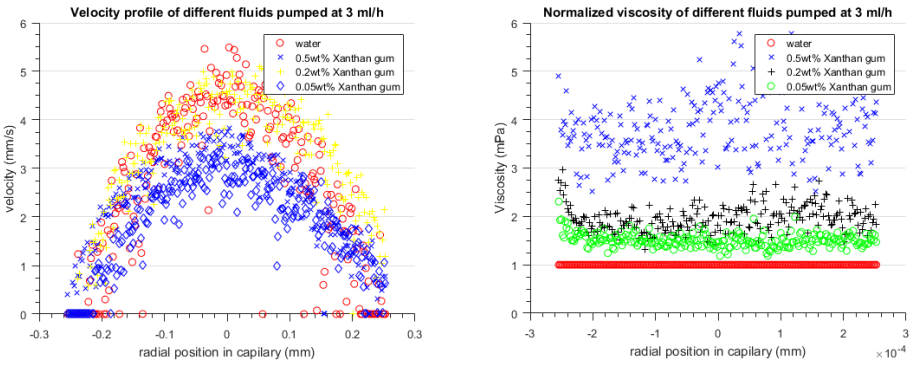


(a) velocity Profile

(b) normalized viscosity profile

Figure A.2: The velocity & normalized viscosity profile for a flow rate of $20\,\mathrm{mL\,h^{-1}}$

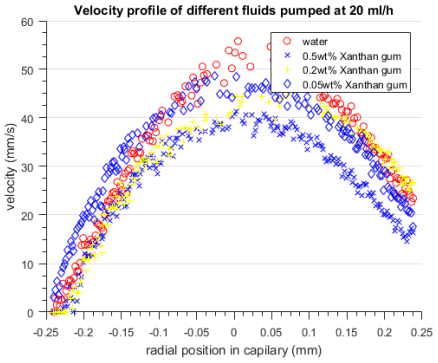


(a) velocity profile

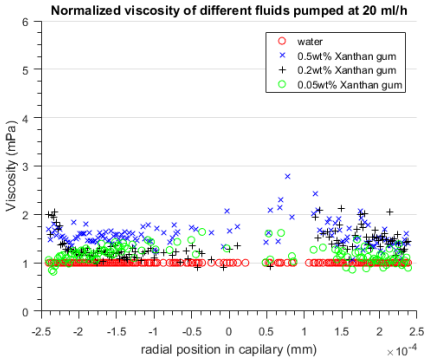


(b) normalized viscosity profile

Figure A.3: *The viscosity profiles for different xanthan gum solution pumped at a flow rate of 3 and* $20\,\mathrm{mL\,h^{-1}}$

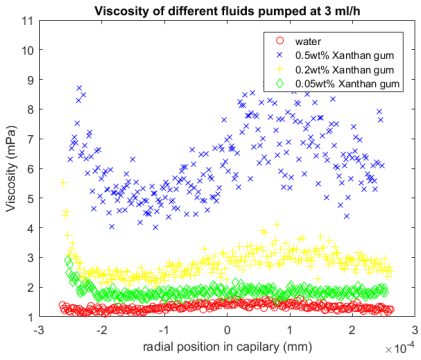


(a) $3\,\mathrm{mL\,h^{-1}}$

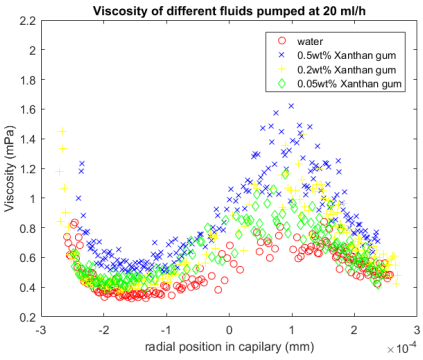


(b) $20\,\mathrm{mL\,h^{-1}}$

Table A.2: *The velocity measured for the intercept of the decay time constants and the first velocity for which the relative error in the viscosity is larger than 10 percent for a flow rate of* $20\,\mathrm{mL\,h^{-1}}$

| concentration (wt%) | $v_{x,decay}(mm/s)$ | $v_{x,95\%confidence-interval}(mm/s)$ |
|---|---|---|
| 0 | 8 | 10 |
| 0.05 | 15 | 16 |
| 0.2 | 12 | 12 |
| 0.5 | 20 | 22 |

Table A.3: *The velocity measured for the intercept of the decay time constants and the velocity from which the errors in the fit become larger than 10 percent for a flow of* $3\,\mathrm{mL\,h^{-1}}$*.When the value is missing there was either no clear intercept between the decay time constants or the error was lower than 10 percent.*

| concentration (wt%) | $v_{x,decay}$ | $v_{x,95\%confidence-interval}$ |
|---|---|---|
| 0 | - | 2 |
| 0.05 | - | - |
| 0.2 | 4 | 2 |
| 0.5 | 2 | 1 |

## A.3 Storage and Loss moduli

Figure A.4: *The storage and loss modulus of xanthan gum solutions*

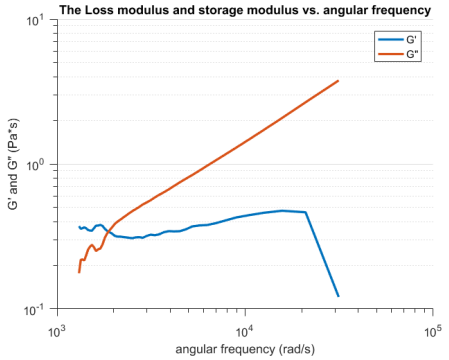


(a) *0.05 wt% xanthan gum*

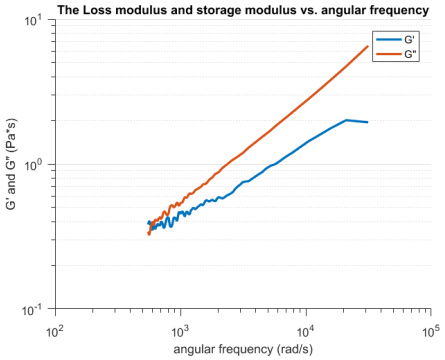


(b) *0.2 wt% xanthan gum*

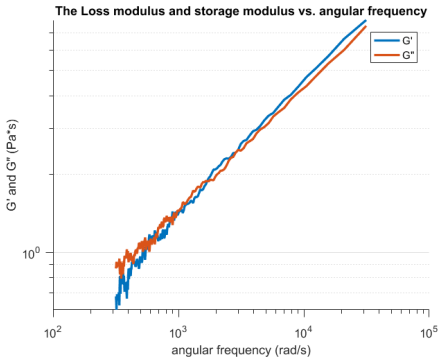


(c) *0.5 wt% xanthan gum*

# B | Microrheology Method

To obtain viscoelastic parameters from the autocorrelation data first the Mean Square Displacement (MSD) must be obtained from the autocorrelation. The relation between the MSD and the diffusion coefficient is:

$$MSD = 2dDt \tag{B.1}$$

In which $d$ is the dimension, which is in this case 3 because the average particle movements are measured in a volume, $D$ is the diffusion coefficient of the particles and $t$ is the time. The normalized autocorrelation function can be rewritten to obtain a function for the MSD:

$$MSD(\tau) = -\frac{6}{2q^2} \ln g(\tau) \tag{B.2}$$

The timeshift $\tau$ is transformed into the angular frequency by:

$$\omega = \frac{2\pi}{\tau} \tag{B.3}$$

The logaritmic slope of the MSD and the inverse angular frequency is needed to evaluate how elastic or viscous the solution is. For a purely elastic solid this slope is equal to zero and for a purely viscous fluid this slope is equal to one.[15]

$$\alpha(\omega) = \frac{d \ln MSD(1/\omega)}{d \ln 1/\omega} \tag{B.4}$$

It has been found that from these equations the complex modulus ($G^*$) can be calculated and with this property the loss ($G''$) and storage modulus ($G'$) can be calculated:

$$G^*(\omega) = \frac{k_b T}{\pi a MSD(1/\omega)\Gamma(\alpha(\omega)+1)} \tag{B.5}$$

$$G'(\omega) = \cos(\pi\alpha(\omega)/2) \tag{B.6}$$

$$G''(\omega) = \sin(\pi\alpha(\omega)/2) \tag{B.7}$$

In these equations is $\omega$ the angular frequency and $\Gamma$ is the Gamma function that can be written as:

$$\Gamma(n) = (n-1)! \tag{B.8}$$

Finally with these parameters the complex dynamic viscosity can be calculated:

$$\eta^* = \sqrt[2]{\frac{G'^2 + G''^2}{\omega^2}} \tag{B.9}$$

This method was described for a Dynamic Light Scattering device in [16] and it was adapted to suit it for the OCT data.